ORCA-Fusion

Gen III Scientific CMOS Camera

TECHNICAL NOTE

Version 1.2 / November 2018

HAMAMATSU

PHOTON IS OUR BUSINESS

Hamamatsu Photonics K.K.

Table of Contents

The First Gen III Scientific CMOS Sensor

The ORCA-Fusion, Hamamatsu's newest member of the ORCA Family of scientific cameras, utilizes a custom scientific CMOS (sCMOS) sensor designed from the ground up for low-light quantitative imaging. By implementing a custom pixel design in this sensor and by using state-of-the-art semiconductor processes we've greatly improved pixel read noise, read noise uniformity and linearity. With these improvements we've achieved our goal of creating a camera that outputs beautiful images and quantitative data directly from the camera, especially in low-light conditions. We consider this the first Gen III sCMOS sensor because the fundamental pixel design is unique and the read noise characteristics surpass existing technology, including well-accepted front-illuminated Gen II sCMOS and newly released back-side illuminated sCMOS. In this TechNote, we will describe the innovative features of our ORCA-Fusion and discuss the advantages these features bring to low-light scientific imaging. Since we have significant experience with Gen II sCMOS, CCDs and EMCCDs, we will also highlight when and how the new ORCA-Fusion can outperform these types of detectors and why data that is innately quiet provides the best data for quantitative and computational imaging techniques.

Read Noise and Read Noise Uniformity

The ORCA-Fusion is designed to provide the best low-light application performance of any sCMOS camera available. To achieve this, we focus on two parameters that are especially relevant to camera performance in photon-starved conditions: read noise and read noise uniformity. The importance of low read noise for low light signal detectability is well known and relatively easy to appreciate: the lower the noise floor the lower the threshold for detecting signal. But the importance of read noise uniformity is a less discussed parameter that has only come to the forefront with the advent of sCMOS cameras, due to the nature of CMOS structure. The following sections define read noise and read noise uniformity in CCD versus CMOS and discuss how these parameters impact low light imaging.

CCD and CMOS sensor structure

To understand the significance of read noise in imaging, it's first necessary to review how digital images are formed in both CCD and CMOS. The basic principle is the same: incoming photons are converted to (photo) electrons via the photoelectric effect in the sensitive layer of the silicon substrate. This electron charge is next converted to a voltage via a floating diffusion amplifier (FDA). Voltage is then amplified again and converted to a digital signal through an analog to digital converter (ADC). CCD and CMOS differ in the on-chip location where each of these steps happen. Ultimately, an image is formed when the charge from each pixel is converted to a digital signal; this process is called read out.

In a CCD, read out happens serially for the entire array. Charge in each pixel is transferred from pixel to pixel in columns and then to a horizontal register. Every pixel is then read out through a single charge conversion, amplification and digitization circuit (Figure 1). In contrast, each CMOS pixel has an FDA, so the charge is converted into a voltage within each pixel and then additional amplification and analog to digital conversion is achieved in column ADCs. In both CCD and CMOS, a process called correlated double sampling (CDS) happens just before the final amplification and digital conversion that helps reduce noise and compensate for pixel offsets and drift.

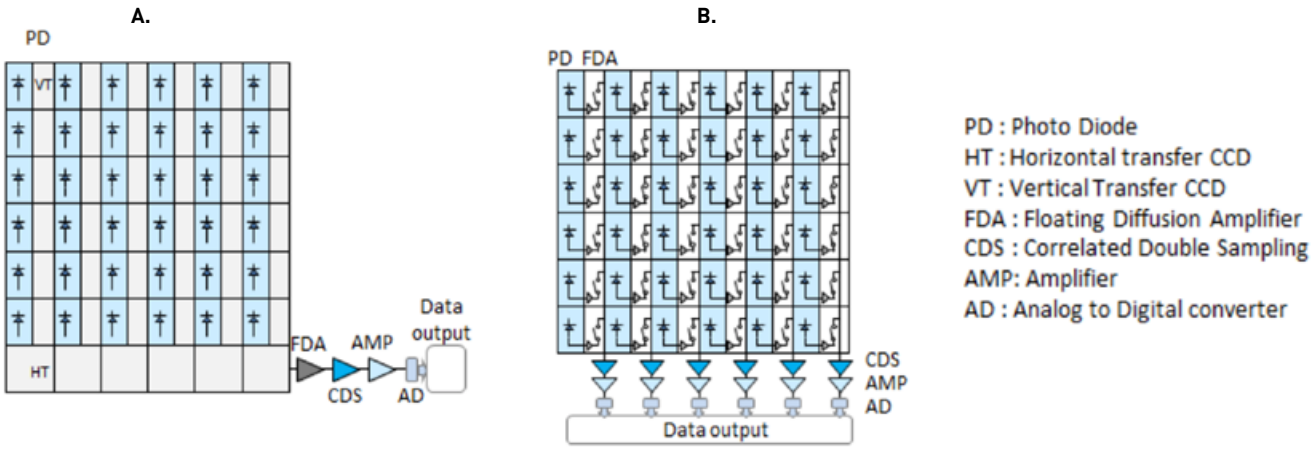

Figure 1. Pixel structure and read out pathway in (A) CCD and (B) CMOS.
CCDs and CMOS are both arrays of photodiodes that are able to detect light by converting photons into electrons. The difference in structure between these two technologies leads to important differences in performance and features. In a CCD, the pixel structure is designed to manage the signal in the charge domain. So all the pixels detect photons as (photo) electrons and the electrons are moved through the sensor for read out. That electron charge is then converted to a digital signal through a single path that includes a floating diffusion amplifier (FDA), a correlated double sampling (CDS) process and finally another amplifier to an analog to digital converter (ADC). This one read out path means that there is a high degree of uniformity among all the pixels. CMOS structure also detects photons as photoelectrons but this charge is immediately converted to a voltage within each pixel by an FDA. That voltage is then converted to digital units through column CDS, amplifiers and ADCs. Because CMOS pixels are read out in parallel, the overall speed of each electrical component can be slow, keeping the read noise low, but the total read out speed and, therefore, frame rates are still fast. The tradeoff is that there can be non-uniformity among CMOS pixels. The Gen III ORCA-Fusion was designed to specifically improve pixel read noise uniformity.

Read noise and read noise uniformity

The entire read out progression of detecting, converting, moving and digitizing the photoelectrons introduces noise, termed "read noise" into the digital image. In both CCD and CMOS, a camera's read noise spec in e- rms defines the read noise of the entire array and is calculated as the root mean square (rms) of the temporal read noise for each pixel. A pixel's temporal read noise is calculated by measuring the standard deviation of that pixel from a series of ~1000 dark images. Since CCD read out happens through a single read out chain, the temporal read noise of each pixel is very nearly identical, and CCD cameras are adequately characterized by a single read noise value. In other words, the variation of a single pixel's read noise in time will have a Gaussian distribution and this distribution is the same as if the variation is measured from many pixels in a single frame after subtracting the dark offset. However, in CMOS, since each pixel has its own charge to digitization chain, read noise must be characterized more carefully. In fact, neither the temporal read noise of an individual pixel, nor the rms read noise of the array fully characterizes the variation in read noise among pixels. A histogram of temporal pixel read noise of an entire frame will show a distribution with a long tail. This tail reflects the non-uniformity of temporal read noise within a CMOS sensor within the read noise spec.

An example of a read noise histogram is shown in Figure 2. As you can see, histograms tell a more complete story of CMOS read noise than a single number. Figure 2 shows the read noise histogram for two theoretical cameras, each with a read noise specification of 1.4 e- rms. In this example, Camera A has no pixels with read noise above 8 e- and Camera B has many pixels above 8 e-. If you were choosing between these two cameras there is no way to know from the rms read noise specification that there is this big difference unless data regarding read noise distribution was provided.

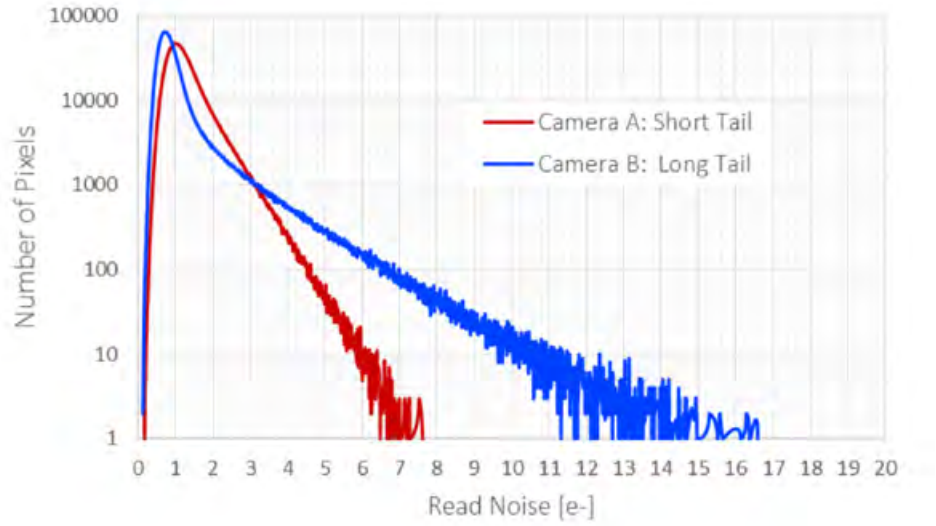

Figure 2. Read noise histogram provides insight into sensor uniformity. Because of the structure of CMOS sensors and the way camera read noise is calculated, any CMOS camera read noise spec in e- rms provides relevant but incomplete data. CMOS cameras, with pixel based charge to voltage conversion, show greater pixel to pixel variation and that is only fully revealed in read noise histograms. In the figure above, simulated data from two hypothetical cameras is shown. Both cameras have a read noise spec of 1.4 e- rms. But a log-linear histogram (Bin size = 0.01 e- rms) of the measured temporal read noise for each pixel shows that one camera has a significantly longer tail of noisy pixels than the other. In this graph, the overall shape of the Camera B (blue) curve resembles the read noise tail of front and back illuminated Gen II cameras. Due to investment in custom pixel design, the Gen III ORCA-Fusion has a narrower distribution and a shorter tail, similar to Camera A (red).

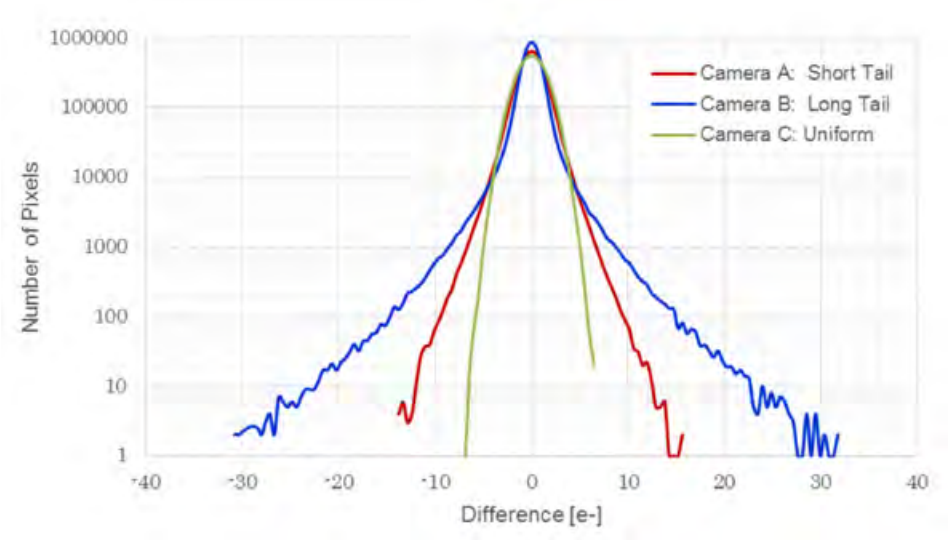

Figure 3. Histogram of the pixel output from a single dark image for three simulated cameras. The distribution in the camera output in each pixel in a single dark frame provides a quick glimpse at the extent of read noise heterogeneity. On the x-axis, dark output shows the fluctuation in signal above and below the camera's offset. The y-axis shows the number of pixels with this value. In this figure, all simulated cameras have a read noise spec of 1.4 e- rms, but Camera B (blue), has large distribution similar to Gen II sensors, both front and back illuminated, Camera A (red) has a narrow distribution similar to the ORCA-Fusion in quiet mode. Camera C (green) simulates the Gaussian distribution of the output of a CCD assuming all pixels have the same 1.4 e- read noise. For measured dark offset intensity data from Gen II and ORCA-Fusion sCMOS cameras see Table 1 below.

While histograms are visually informative, their practical usefulness is limited. For the ORCA-Fusion, we have chosen to present the data from a single frame in a more digestible format, shown in Table 1. Consider a typical Gen II sCMOS camera with 1.4 e- rms read noise and 4.2 million pixels. Within a single frame of 4.2 million pixels, as many as 1.3% or 54,000 pixels could vary from the dark offset by > 6 e- and furthermore, as many as 1000 pixels will have readings of > 20 e-. At high light, shot noise of the signal dominates and the high read noise pixels are mostly irrelevant. But in low light, these noisy pixels can disrupt everything from auto look-up tables for display, to x-z and y-z image projections and 3D reconstructions. Furthermore, these pixels must be specially considered in single molecule precision localization algorithms where the bright "noise" can skew localization results (Huang, F., et al., Nature Methods, DOI:10.1038/NMETH.2488 (2013)). In spite of these pixel uniformity issues, CMOS sensor have been widely accepted because they deliver major speed, field of view and other performance benefits over CCDs and even EM-CCDs. In some cameras, the work around for these high read noise pixels has been to offer "noisy" or "dynamic" pixel filters than can smooth the data based on the surrounding pixels when intensities are low. Because it's critical for accurate quantification, Hamamatsu's dynamic pixel filter in the ORCA-Flash4.0 is fully documented and user controllable, with three levels of correction and an "off" option. The Gen III ORCA-Fusion was designed to minimize pixel to pixel variation and does not require any noisy pixel filters. Even in fast mode with 1.4 e- rms noise, only 0.25% of ORCA-Fusion pixels vary from the dark offset by > 6 e- and in ultra-quiet mode with 0.7 e- rms this value drops to 0.07% and only 2 pixels are >12 e-. The uniformity of the ORCA-Fusion is unique and combined with very low read noise overall improves and simplifies quantitative low-light imaging.

Camera	ORCA-Flash4.0 V3		ORCA-Flash4.0 V3		ORCA-Fusion		ORCA-Fusion	
Mode	Slow		Slow		Fast		Standard	
Read Noise	1.4 e- rms		1.4 e- rms		1.4 e- rms		1.0 e- rms	
	Noise Pixel Correction OFF		Noisy Pixel Correction ON-Low		No Noisy Pixel Correction Needed		No Noisy Pixel Correction Needed	
Threshold [e-]	Pixels	Ratio [%]	Pixels	Ratio [%]	Pixels	Ratio [%]	Pixels	Ratio [%]
2	330050	7.8690	291030	6.939	667696	15.919	225676	5.381
4	108920	2.5969	74274	1.771	69071	1.647	24034	0.573
6	54195	1.2921	25194	0.601	10412	0.248	2826	0.067
8	29602	0.7058	5585	0.133	1489	0.035	286	0.007
10	16472	0.3927	1439	0.034	193	0.005	26	0.001
12	9246	0.2204	610	0.015	23	0.001	2	0.000
14	5310	0.1266	295	0.007	3	0.000	0	0.000
20	1069	0.0255	37	0.001	0	0.000	0	0.000

Table 1. Measured distributions of absolute dark output after pixel offset subtraction from a single frame in Gen II, Gen II with correction and Gen III ORCA-Fusion camera. This table addresses the question of pixel read noise uniformity in single frame with measured data. The dark offset of a camera is a known and set value. In a dark image, measuring pixels with values both above and below the offset is a way to examine read noise uniformity. For each camera and mode, we display the number of pixels with an absolute value of the difference between the dark reading and the offset at or above a threshold value. Even when the cameras are compared in modes with identical camera read noise of 1.4 e- rms, only 0.25% of the pixels in the ORCA-Fusion have readings 6 e- or greater from the offset, while the Gen II ORCA-Flash4.0 V3 (and likely all other camera made with this same sensor) has 5x more pixels at this level. In low light scenarios, these noisy pixels can disrupt auto-scaling, x-z projections and 3D renderings, and single molecule precision localization algorithms. The ORCA-Fusion provides clean image data for whatever post-acquisition processing is needed.

What does read noise non-uniformity look like in an image?

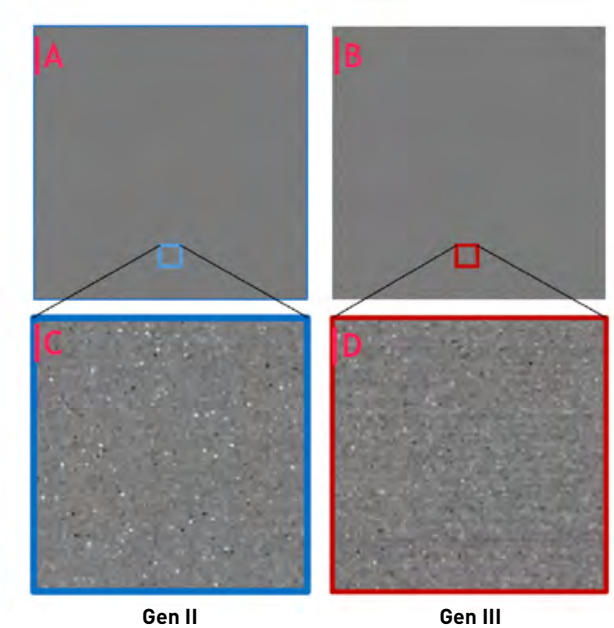

Figure 4. Comparison of dark images from Gen II and Gen III sCMOS. In a dark image that is scaled appropriately, it's possible to see noisy pixels. In Gen II sensors, this noise is visible as a salt and pepper effect, especially when viewing live dark images. These static dark images compare the ORCA-Flash4.0 V3 (A and C) to the ORCA-Fusion (B and D). With the improvement in the sensor design to reduce read noise and increase read noise uniformity the ORCA-Fusion dark images have much less of this salt and pepper display of read noise. Panel A: ORCA-Flash4.0 V3. Panel B: ORCA-Fusion. Panel C: Zoom of 100x100 pixels of ORCA-Flash4.0 V3. Panel D: Zoom of 100x100 pixels of ORCA-Fusion. The look-up tables of all images are set to the same values for easy comparison.

Implications of Read Noise and Read Noise Uniformity

Read noise and signal to noise ratio

Pixel signal to noise ratio (SNR) is a standard metric used to express camera sensitivity. For CCDs and sCMOS, pixel SNR is calculated as Equation (1). Note that this equation assumes the exposure time is short, so the dark noise becomes small and negligible, and does not need to be included in the equation.

$$SNR = \frac{(QE \times S)}{\sqrt{QE \times (S + I_b) + N_r^2}}$$

Equation 1. SNR equation for CCD and CMOS. QE is quantum efficiency (%/100), S is input photon number (photons / pixel / s), I_b is background, N_r is read noise (e- rms). This equation assumes dark noise is not a significant contributing factor for SNR due to short exposures and low dark current. For more info on SNR, please see Hamamatsu's ORCA-Flash4.0 white paper called "Changing the Game" and for details on SNR in EM-CCDs please see below.

In this equation, both QE and read noise contribute to camera "sensitivity." Keep in mind however, that even a perfect camera with 0 e- read noise and 100% QE, images will still have noise from shot noise. So a low light image always "looks" noisy regardless of the camera (see below). Calculating SNR (or alternatively contrast to noise ratio) gives a quantitative versus qualitative appreciation for the impact of QE and read noise at low light.

Low camera read noise improves low-light image quality

Biological samples are not cooperative when it comes to providing a specific output photon number. Figure 5 demonstrates the visual impact of read noise and QE. By simulating images at low light with increasing camera read noise and two QEs, a hypothetical 100% QE and 80% QE, it's possible to see that at low-light (average 5 photons/pixel) visual image quality is affected by read noise. So if what you are trying to do is see dim samples, and you need to choose between low read noise and high QE, low read noise can provide better visual contrast.

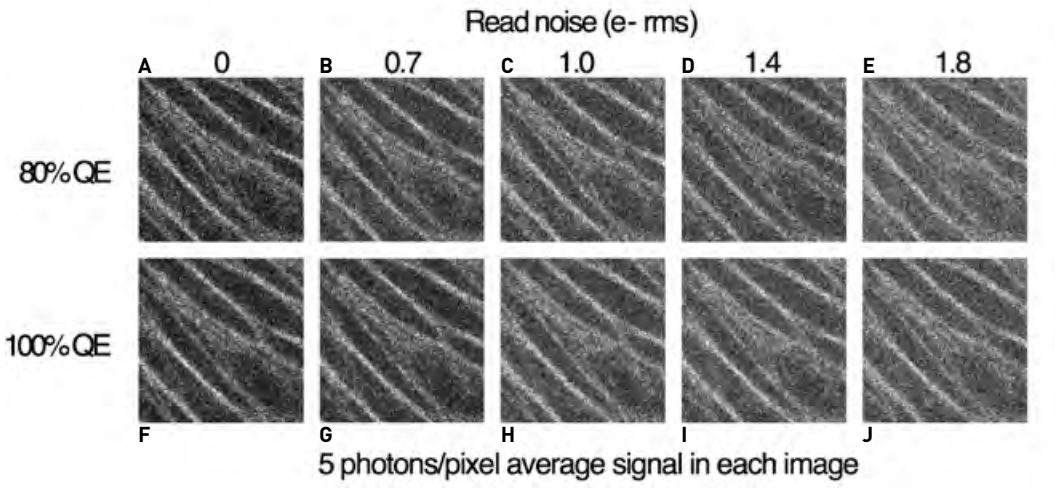

Figure 5. Visual image quality depends on light levels, read noise and QE. From these simulated images it's possible to see how multiple parameters affect image quality in low light. Panels A and F have 0 read noise at 80% and 100% QE respectively. In these images, the noise is exclusively due to shot noise. So even with a "perfect camera," without enough light, images are noisy. When camera noise is added to a system, even with 100% QE, visual contrast becomes worse. Of course the best scenario is to have both high QE and low noise, but when this is not an option, low read noise can provide better visual image quality in low light scenarios. All images scaled so that the minimum LUT is 0.15% above the darkest pixel and the max LUT is 0.15% below the brightest pixel.

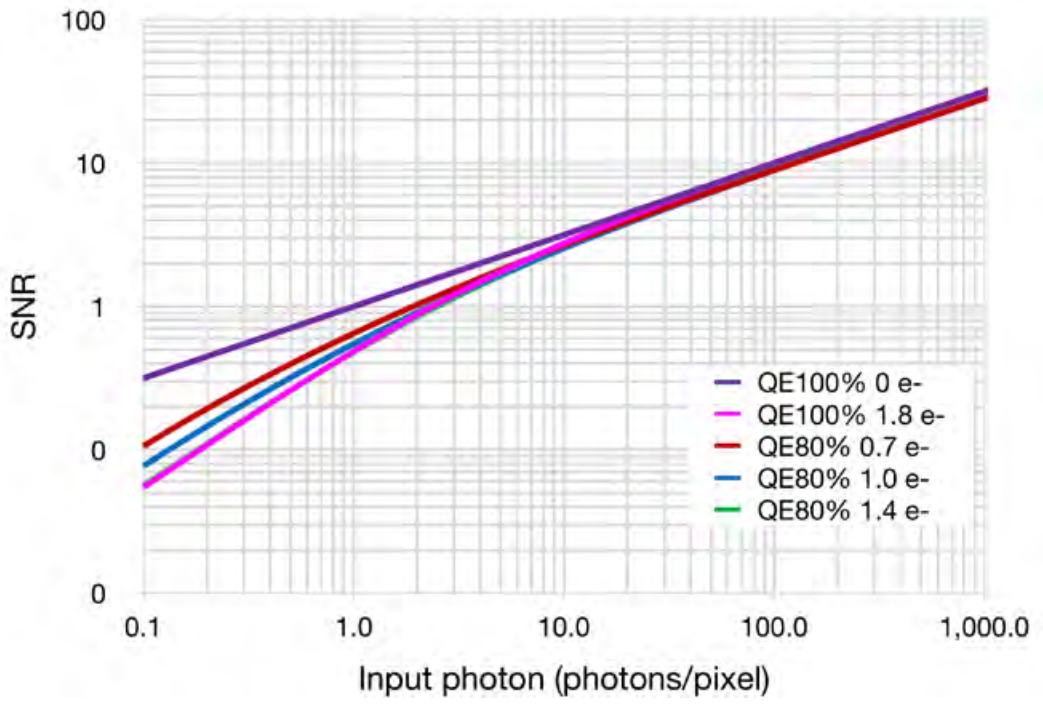

Figure 6. SNR curves show impact of read noise at low light. Equation 1 above shows how to calculate SNR for a pixel with a given intensity. But to appreciate the impact of the various factors on SNR, it's useful to plot SNR as a function of input light intensity. This graph shows five hypothetical cameras including a perfect camera with 0 noise and 100% QE. The point here is to visually display how read noise and QE impact SNR curves. At low light, read noise dominates the equation and small reductions in read noise noticeably improve SNR. A camera with 80% QE and 0.7 e- rms read noise can provide better SNR than a camera with 100% QE with 1.8 e- rms noise at fewer than 7 photons per pixel. Although most samples can provide more signal than 7 photons per pixel, having the option to obtain quality images at low light, means that experiments can be designed to specifically reduce light dose to the sample.

To complement Figure 5 images with quantitative data, Figure 6 shows SNR plots for 5 simulated cameras. Such simulated SNR plots are commonly used to show the light intensity where a camera with certain spec is either read noise limited or shot (signal) noise limited. To be shot noise limited means that the noise resulting from the signal is greater than the noise from the camera. In an SNR plot, the shot noise limited regime begins at the light level where the plot trasitions from a curved to a straight line. Figure 6 shows that at low light, a camera with 80% QE, can outperform a camera with 100% QE if the read noise for the 80% QE camera is better. In the shot noise dominated region, higher QE will give higher SNR.

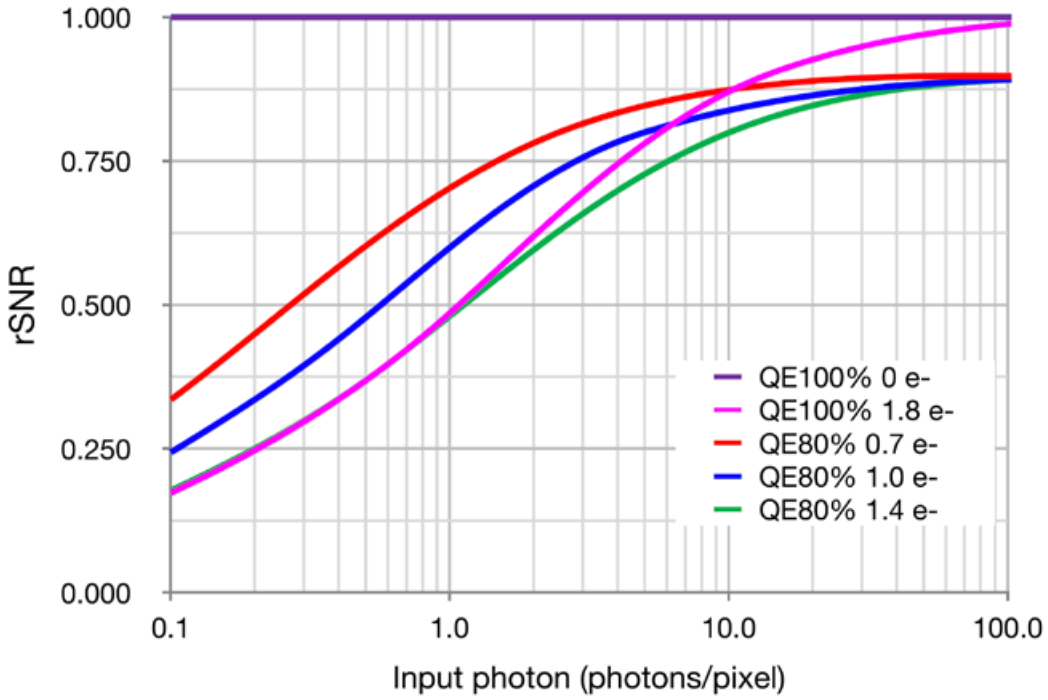

Figure 7. Relative SNR curves show importance of read noise at low light. Figure 6 shows standard SNR curves. To truly see details of SNR at low light, it's useful to make SNR calculations relative to a perfect camera with 100% QE and 0 read noise. This graph shows the same four hypothetical cameras relative to a perfect camera. Seemingly small differences in read noise offer large improvements in SNR at ultra-low light levels. At higher light levels, higher QE does results in higher SNR, primarily because the SNR is now shot noise limited, not read noise dependent.

The format of the SNR graph makes it difficult to see subtle difference at low light. To improve visualization of low light SNR curves, we developed the rSNR plot. An rSNR graph simply makes all the SNR data relative to a perfect camera with 0 read noise and 100% QE. Figure 7 is the data in Figure 6 presented as a rSNR. Now it's possible to see fine differences in performance even when read noise changes from 1.0 to 1.4 e- rms and QE remains the same. Also, while SNR is important, this pixel based measurement does not consider read noise uniformity for the overall image quality.

Binning and other practical advantages of low read noise

Switching from CCDs to CMOS for scientific imaging has many advantages. Lower read noise, larger field of view and faster frame rates are key to sCMOS adoption. But binning is one feature of imaging that is fundamentally altered by the structure of CMOS sensors. In CCDs, charge from the binned pixels is combined before readout and is therefore noiseless. Binning *n* pixels results in *n* times the signal with the same read out noise. Thus, at low light, a binned CCD pixel has *n* times the SNR of the unbinned pixels. For example, a 2x2 bin in a CCD collects 4x more light with no additional increase in read noise and therefore has a 4x increase in SNR. But in CMOS, binning is done after digitization, typically in an on-board FPGA. Binning *n* CMOS pixels increases the signal by *n* and the noise by $\sqrt{n}$. So in sCMOS, there is only 2x increase in SNR when 2x2 binned. It's important to note that in bright light scenarios, the SNR for binned CCD pixels (but not CMOS) must also consider shot noise.

For Gen II sensors with read noise ranging from 1.4 to 1.8 e- rms, 2x2 binning doubles the read noise and reduces the usability in low light, particularly for high magnification applications where large pixels are more appropriate. But the ORCA-Fusion in ultra-quiet mode has read noise of just 0.7 e- rms. In this mode, with 2x2 binning, the noise floor is equivalent to an ORCA-Flash4.0 but the pixel size is now 13 µm, quadrupling the signal. Of course there is still a loss of spatial resolution but for some experiments this is a perfectly reasonable tradeoff. With low read noise, binning is now a highly viable and versatile option for researchers who sometimes need speed and resolution and other times need larger pixels for maximum signal collection in low-light. The ORCA-Fusion does both in a single camera, making it particularly well suited for both lower magnification (60x and under) and higher magnification applications (100x or more), where large pixel image sensors have traditionally been used.

In live cell biological applications, low read noise can be a life saver for cells. Illumination dose, both in terms of intensity and time, can induce phototoxic effects. Anyone working on live cell imaging knows that the best way to reduce phototoxicity induced cell death is to keep the light dose low. The low read noise of the ORCA-Fusion means that experiments can be designed with shorter exposures and/or less intense illumination since this camera can deliver similar or better SNR and image quality with fewer photons.

Comparing EM-CCDs to the ORCA-Fusion sCMOS

Electron multiplying CCDs (EM-CCDs) became the camera of choice for low-light imaging shortly after their introduction in 2001. EM-CCDs were successful because electron multiplication gain rendered read noise irrelevant, even with low-light samples. EM-CCDs became the low-light imaging stars because of this on-chip gain, relatively fast frame rates (because they had few pixels) and high QE. The effect of the gain was to amplify the signal above the read noise. But there were tradeoffs for this benefit. In addition to reducing dynamic range, the gain added an additional noise factor (electron multiplication noise) to the signal so in SNR equations the high QE was effectively halved. An often overlooked property of EM-CCDs that allowed them to excel in low light was simply their large pixel size. When compared directly to standard interline CCDs of the time with 6.45 µm pixels and later to sCMOS with 6.5 µm pixels, the 16 µm pixel of an EM-CCD collected more light. Even with these caveats, 512 x 512 EM-CCDS using the E2V CCD97 chip were suited to extremely low light applications, especially those with little or no background signal like TIRF and Spinning Disk Confocal. But with the introduction of Gen II front and back illuminated sCMOS and now the Gen III ORCA-Fusion, the range of applications for which the EM-CCD is the best camera choice continues to narrow.

$$SNR = \frac{(QE \times S)}{\sqrt{F_n^2 \times QE \times (S + I_b) + \left(\frac{N_r}{M}\right)^2}}$$

Equation 2. SNR Equation for EM-CCDs. The standard SNR curve for CCDs and sCMOS as shown in above in Equation 1 must be modified for EM-CCDs, because EM-CCDs have Gain (M) and Excess Noise Factor (F). Again, this equation assumes fast frame rates and short exposure times since it does not include dark current noise. Using this equation it's now possible to compare SNR from EM-CCD to sCMOS as shown below in Figure 8. QE is quantum efficiency (%/100), S is input photon number (photons / pixel / s), F_n is excess noise factor (EM-CCD F_n = 1.4, others F_n = 1), I_b is background, N_r is read noise (e- rms), M is multiplication gain of EM-CCD (M=1 for CCD or sCMOS). For more detailed info please see our ORCA-Flash4.0 White Paper.

When Gen II sCMOS were introduced, many long-time EM-CCD users explored making the switch to sCMOS. A fundamental problem with any comparisons was the big difference in pixel size. A 16 µm pixel has 6x more area than a 6.5 µm pixel and appears to be more "sensitive" because it collects more light. The correct way to compare these cameras was to optically match pixel size by adding a 2.5x magnifying C-mount adaptor to the EM-CCD. In theory this is simple, but in practice it rarely happened. The typical comparison between sCMOS and EMCCD was done by binning the sCMOS 2x2 to emulate a 13µm pixel, an insufficient but better approximation of the 16 µm EM-CCD pixel. And, in some cases this was good enough. But, as discussed above, binning on a CMOS increases the signal by 4x but also increases the read noise by 2x. And this is where these comparisons fell apart. The advantage of EM-CCD was the low relative read noise. Gen II sCMOS have low read noise (1.4 e- to 1.8 e- rms) but when this is doubled in 2x2 binning, Gen II sCMOS cannot compete with EM-CCD in lowest light because the noise floor is just too high.

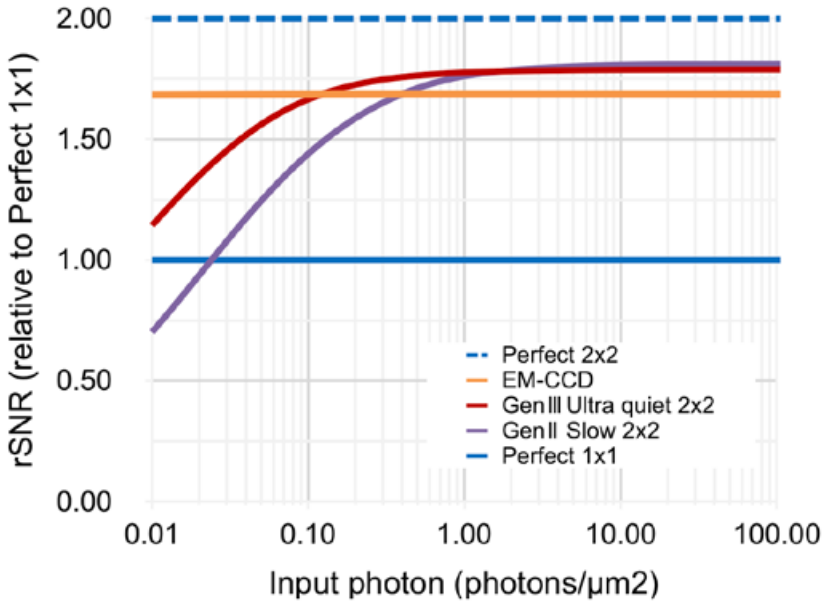

Figure 8. Relative SNR (rSNR) for ORCA-Fusion and ORCA-Flash4.0 V3 binned 2x2 to EM-CCD. Even though there is a large difference in pixel sizes, it's common for comparisons of EM-CCD and sCMOS to be done without optically matching pixels. This paradigm puts the sCMOS at a disadvantage because its smaller pixels collect less light. Often the quick solution to the pixel size issue is to bin the 6.5 μm pixel of the sCMOS to more closely match the 16 μm pixel of the EM-CCD. Unfortunately this also disadvantages sCMOS because in 2x2 bin the read noise is doubled. But, in the ORCA-Fusion, especially in ultra-quiet mode, the read noise is low enough that a 2x2 bin can have advantages. Even with 34% less area than the EM-CCD pixel, the ORCA-Fusion 2x2 SNR exceeds the EM-CCD SNR at just 0.12 photons per μm^2. This photon number corresponds to 30 photons per pixel at EM-CCD of 16 μm. For the ORCA-Flash4.0 in 2x2 bin this crossover point is at 0.38 photons per μm^2. This photon number corresponds to 97 photons per pixel at EM-CCD of 16 μm.

But the ORCA-Fusion Gen III sCMOS changes this story because it can be operated in ultra-quiet mode with just 0.7 e- rms. Figure 8 shows a comparison of EM-CCD to an ORCA-Fusion and ORCA-Flash4.0 V3 in 2x2 bin. Even with the disadvantage of having 34% less area than the EM-CCD pixel, the SNR of the ORCA-Fusion with 2x2 bin exceeds the EM-CCD SNR at just 0.12 photons per μm^2 which corresponds to 30 photons per pixel on the 16 μm EM-CCD.

For this reason, the ORCA-Fusion offers unprecedented versatility. In applications that can sacrifice spatial resolution in exchange for signal, the ORCA-Fusion in 2x2 ultra-quiet mode will provide as good or better SNR than an EM-CCD and has a binned pixel size of 13 μm that is better matched to Nyquist sampling theorem at 60x and 100x than an EM-CCD. But when the application calls for high resolution, the ORCA-Fusion running in 1x1 mode still excels at low light and outperforms EM-CCD SNR at 12 photons per pixel (when optically pixel matched). If speed is an issue, using a region of interest with 2x2 bin can increase the frame rate. In ultra-quiet mode with 2x2 bin, a region of 1152 (h) x 200 (v) can deliver over 30 fps, the typical frame rate of an EM-CCD.

Beyond Noise: Other Features of the Gen III ORCA-Fusion

Read noise and uniformity are just two features of the camera that contribute to overall image quality and camera performance. Since we designed the ORCA-Fusion Gen III sCMOS sensor from the ground up, we were able to consider multiple other parameters that in combination offer excellent performance for a variety of applications and conditions.

Single AD convertor

The Gen III sensor in the ORCA-Fusion has a single analog-to-digital converter. This means that achieving linearity with this sensor is uncomplicated. For comparison, both front and back-illuminated Gen II sCMOS sensors use separate amplifiers for low light (high gain) and high light (low gain) signals. Each of these amplifiers outputs 11 bits and these outputs are combined within the camera FPGA to achieve a final 16 bit image. Because Gen II high and low amplifier gains have different slopes, the quality of the linearity throughout the full range of intensities is highly dependent on the camera manufacturer's ability to seemlessly integrate these two ADC chains. For this reason, every Gen II camera must have an on-board linearity correction. The tricky part is achieving good linearity where the two amps overlap, around 1,000 – 2,000 e-. If not done carefully, Gen II cameras can show vertical stripes and/or photon transfer curve anomalies just at this range of input photon level.

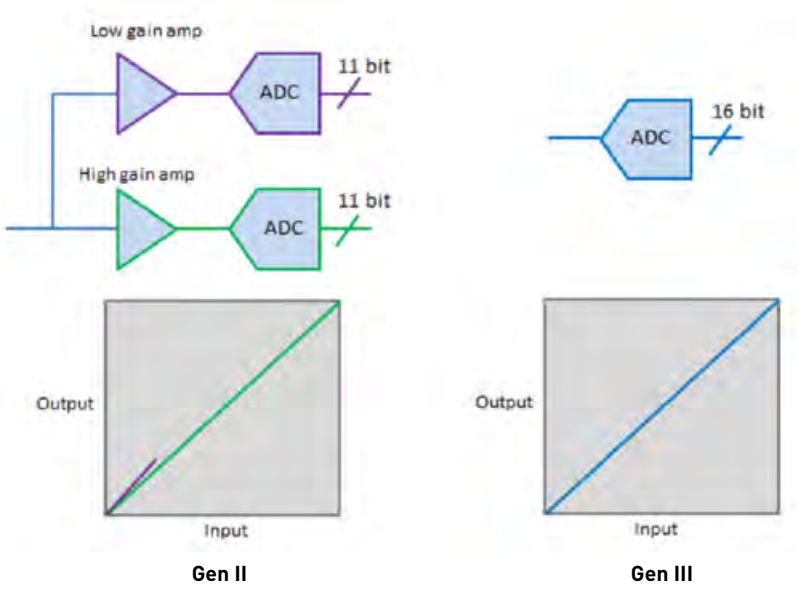

Figure 9. Sensor design improves linearity. Both Gen II front and back-illuminated sensors utilize two 11 bit digitizers that are combined in an FPGA to achieve a full 16 bit image. This design creates complications for camera designers who must first calibrate and then correct the data to achieve linearity across the full range of input light levels. The Gen III sensor uses a single 16 bit digitizer that eliminates this process and means that linearity will be equivalent in low and high light regions of the image.

Speed/noise modes and frame rates

Because read noise arises from slight variations in converting analog signals to digital, faster digitizers typically have higher read noise. Implemeting a multi-speed digitizer in a camera allows for optimization of speed versus noise for given experimental conditions. The ORCA-Fusion camera has three scan speeds: fast, standard (default) and ultra-quiet with 1.4 e-, 1.0 e- and 0.7 e- rms read noise respectively. In fast mode, scan speed is 4x faster than in standard mode. Ultra-quiet mode prioritizes low noise over speed, achieving just 0.7 e- rms with 5.4 fps. Table 2 shows read noise and scan speed data in comparison to Gen II.

Area		GenII		Gen III ORCA-Fusion		
H (pixels)	V (pixels)	Standard	Slow	Fast	Standard	Ultra-quiet
Read Noise e- rms		1.6	1.4	1.4	1.0	0.7
2,304	2,304			88.8 fps	21.1 fps	5.4 fps
2,304	2,048	100 fps*	30 fps*	99.9 fps	23.7 fps	6.1 fps
2,304	1,024			199.6 fps	47.4 fps	12.3 fps
2,304	512			398.4 fps	94.7 fps	24.9 fps

Table 2. Scan Speeds and Read Noise. In CMOS, because readout is multiplexed via per pixel digitization and column amplification, scan speeds are described in terms of overall frame rates (frames per second or fps). Furthermore since parallelization happens in columns in CMOS, scan speeds are increased by regions of interests (ROIs), but only when the ROI is smaller in the vertical direction (i.e. fewer pixels per column). The three scan speeds in the ORCA-Fusion allow for optimal experimental customization by allowing users to prioritize noise versus speed versus field of view. Because the pixel number is higher in the Gen III versus Gen II, the full frame rate is slightly lower but the overall pixel throughput is increased by 12.6%.

Pixel gain and offset uniformity

Pixel uniformity has always been the greatest challenge in creating a CMOS that can satisfy the rigorous quantitative needs of imaging scientist. The primary means of achieving uniformity happen at the level of the pixel design and wafer processing, as we've discussed with read noise uniformity above. Even with the best CMOS designs, there will still be slight differences in pixels when it comes to QE, gain and offset. This is where intelligent camera design and experience with characterizing and correcting pixel perfomance make a difference in the quality and quantitative nature of the image data.

Offset, or "dark signal non-uniformity" (DSNU) describes pixel non-uniformities under dark conditions that are independent of read noise. Figure 10A shows a useful analogy. If distance were measured with a ruler that did not start at 0, the measurement would be incorrect. If a pixel in the dark is not correctly calibrated to 0, then instensity measurements will not be correct. By using masked areas of the chip as a reference, camera engineers can establish a known baseline in absolute dark and apply this to all pixels in the array using the onboard FPGA. Without such a correction, quantitative image analysis would be virtually impossible. DSNU is measured in e- rms and for scientific cameras the value should be less than read noise, since DSNU is most noticeable at low light. For the ORCA-Fusion, DSNU is 0.3 e- rms.

Gain is defined as the conversion factor; it's the slope at which an input photon is converted to a digital number. Each pixel's gain in an sCMOS can be slightly different but this difference is stable and measurable and therefore correctable. The product of pixel dependent QE and gain variation is often

described as photo response non-uniformity or PRNU. The key to correcting PRNU accurately is to map the sensor's output using a very steady and uniform input light. This physical mapping of the variation allows for a quantitative correction to be stored in the camera FPGA and applied to all images. PRNU is typically stable over time although there may be a spatial pattern to the non-uniformity. The spec for PRNU is expressed at % maximum and for the ORCA-Fusion the value is 0.06%. To help understand this spec, imagine three rulers each with different scales as shown below is Figure 10b. If the unit length is incorrect, the absolute measurement is also incorrect, for rules or for pixels. In this example, the mean of the "gain" of the three rulers is 11.9 and each ruler varies from this mean by a calculated percent. The maximum variation is 22%.

For deeper look at PRNU and DSNU and how they are calibrated, please see our poster from 2017 Focus on Microscopy.

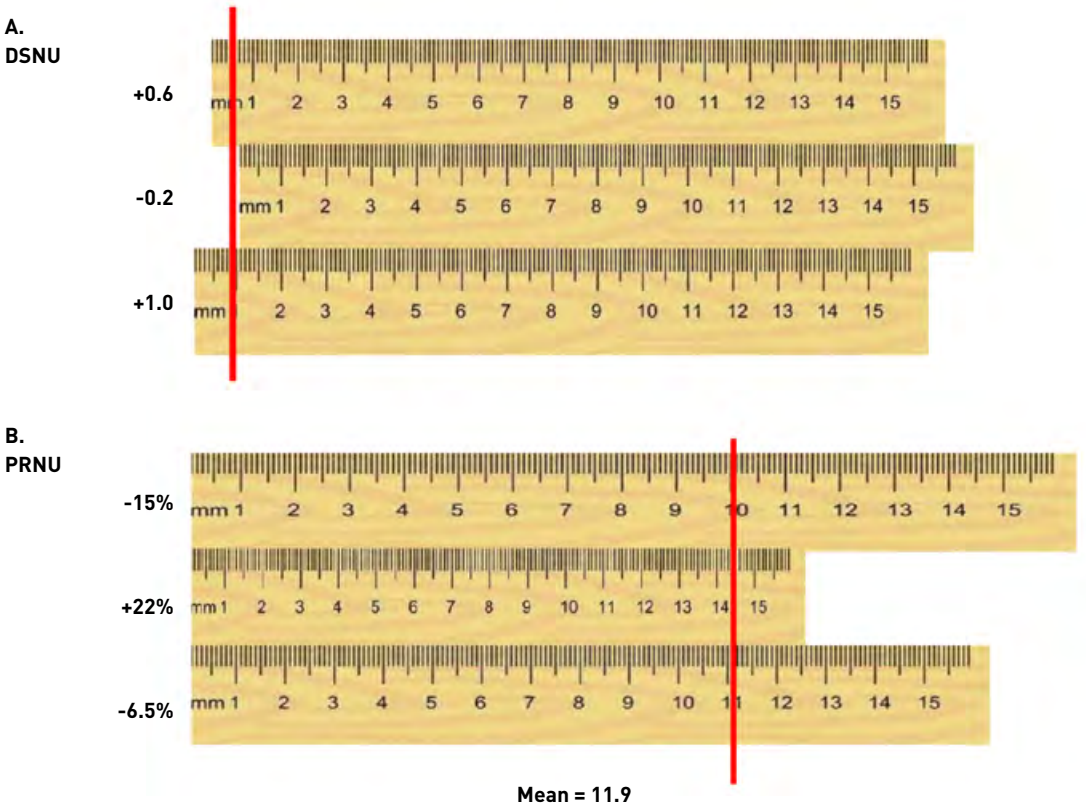

Figure 10. Camera calibrations are similar to standardization of rulers. In Panel A, three rulers with differing starting points are meant to show the impact of variations in pixel offset. Even with no light, a pixel will have a certain intensity value that is deliberately set above zero. This is done to be able to detect both positive and negative noise fluctuations in that pixel. However, all the pixels in an array should start off with the same known offset, otherwise intensity measurements will be inaccurate. This offset correction is stored in the camera FPGA and has the same effect as lining up all the rulers so they start at the same point. Panel B shows three rulers each with a slightly different scale as an analogy for PRNU. This is equivalent to pixels having slightly different gains. The mean gain of the ruler for the point measured is 11.9. The middle ruler has the maximum difference from this mean at 22%. For a detailed explanation of DSNR and PRNU, see our poster from 2017 Focus on Microscopy.

Readout direction

A well-known characteristic of the Gen II front illuminated sensor is that the readout architecture is designed so that the top and bottom half of the chip are read out through separate column amplifiers. A consequence of this design is that in certain imaging paradigms, especially those involving frame averaging (see Figure 11C), it's possible to see the center line. Furthermore to achieve the fastest frame rates with ROIs the ROI had to be positioned evenly around the center. The Gen III ORCA-Fusion sensor reads out in full columns and therefore these Gen II issues are eliminated. Figure 11D shows that even with 20 frame average the image is clean without visible column fixed pattern or center line artifacts.

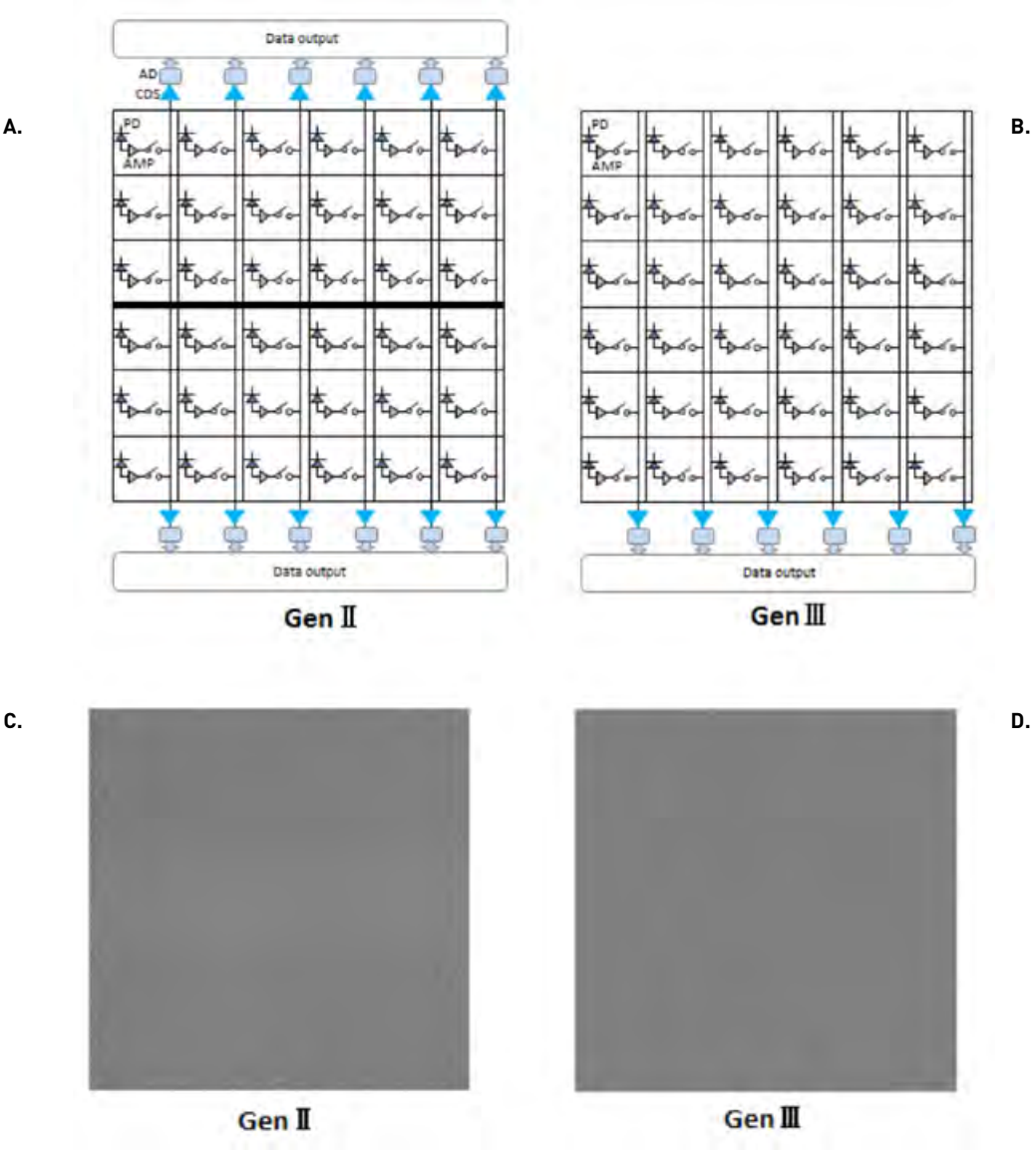

Figure 11. Panels A and B show the read out scheme for Gen II and Gen III sCMOS sensors respectively. Because Gen II front illuminated sensor have a dual column amplifier structure, with frame averaging, the center line of Gen II sCMOS is noticeable (Panel C). With implementation of single column amplifiers, the Gen III sensor eliminates this issue (Panel D). This design has implications for numerous applications especially when using Lightsheet readout mode.

Lightsheet readout mode

Lightsheet readout mode is a patented[1] process developed by Hamamatsu that synchronizes the rolling read out of the sensor with the sweep of a lightsheet. The advantage of this method for lightsheet is that only the sample plane being imaged is illuminated, reducing scatter and improving contrast. Due to the bi-directional column readout of the Gen II front illuminated sensor, lightsheet readout mode in the ORCA-Flash4.0 is limited to 49 fps with a single lightsheet. Synchronized dual lightsheets are needed to achieve 100 fps. But the design of the Gen III sensor, with fast single column amplifiers, it's possible to achieve 100 fps at 2048 vertical pixels with a single lightsheet.

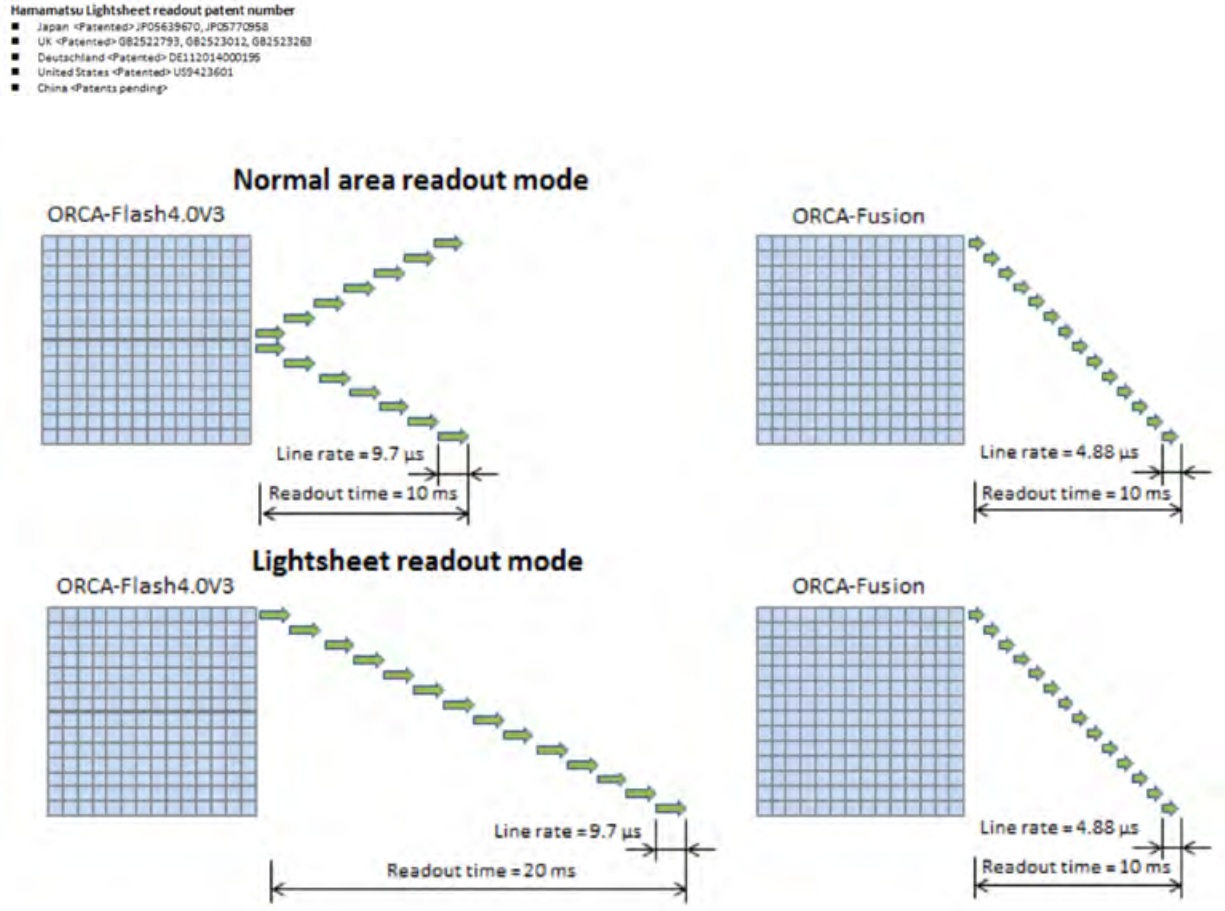

Figure 12. Lightsheet readout mode for ORCA-Fusion. In Normal area readout mode, Gen II front illuminated sensors readout from the center and have single line delay of 9.7 µs. The Gen III Fusion sensor has a single column readout that is about 2x faster than Gen II with a single line read out time of 4.88 µs. This faster speed means that it's possible to achieve 100 fps with a single synchronized lightsheet using the ORCA-Fusion at 2304 (h) x 2048 (v).

H (pixels)	V (pixels)	ORCA-Flash4.0 V3	ORCA-Fusion
2,304	2,304	-	89 fps
2,304	2,048	49 fps (at 2,048 x 2,048)	100 fps

Table 3. Lightsheet readout speeds for ORCA-Fusion vs ORCA-Flash4.0 V3. Even with a larger area, the ORCA-Fusion achieves faster Lightsheet readout due to fast rolling shutter of the ORCA-Fusion.

Pixel size and field of view

For microscopy work, a pixel size of 6.5 µm is a good compromise for resolution and collection efficiency and has been a de facto microscopy standard since the days of CCDs. The Gen III uses that same 6.5 µm pixel dimension but with more pixels, increasing the pixel number to 2,304 x 2,304 or 5.3M pixels. This 25% larger field of view has a diagonal dimension of 21.2 mm, which falls just within the standard objective field number of 22 mm.

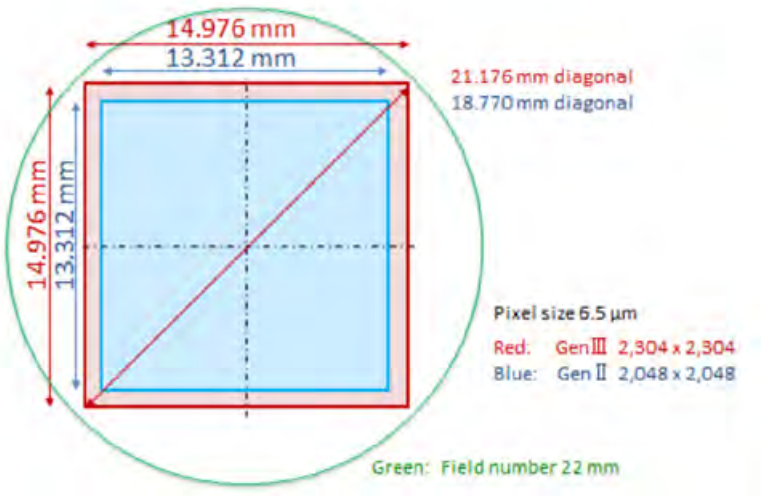

Figure 13. ORCA-Fusion Gen III sensor is 25% larger than Gen II. The Gen III Fusion sensor keeps the same 6.5 µm pixel size as Gen II, but adds an additional 1.1M pixels. The array size of 2,304 x 2,304 pixels has a diagonal dimension of 21.2 mm, just fitting inside the 22 mm field number of standard objectives.

Quantum efficiency

Quantum Efficiency is the percent of photons hitting the sensor that are converted to photoelectrons. QE is an important piece of camera sensitivity and high QEs allow for reduced exposures while maintaining SNR. QE is a wavelength-specific sensor dependent property. Although the Gen III Fusion sensor is not backside thinned (or back illuminated), the QE of the sensor is quite high as far out at 825 nm and as low as 400nm. By maintaining high QE on the wings of the visible spectrum into the UV and NIR, the ORCA-Fusion makes imaging at a range of wavelengths easily accessible.

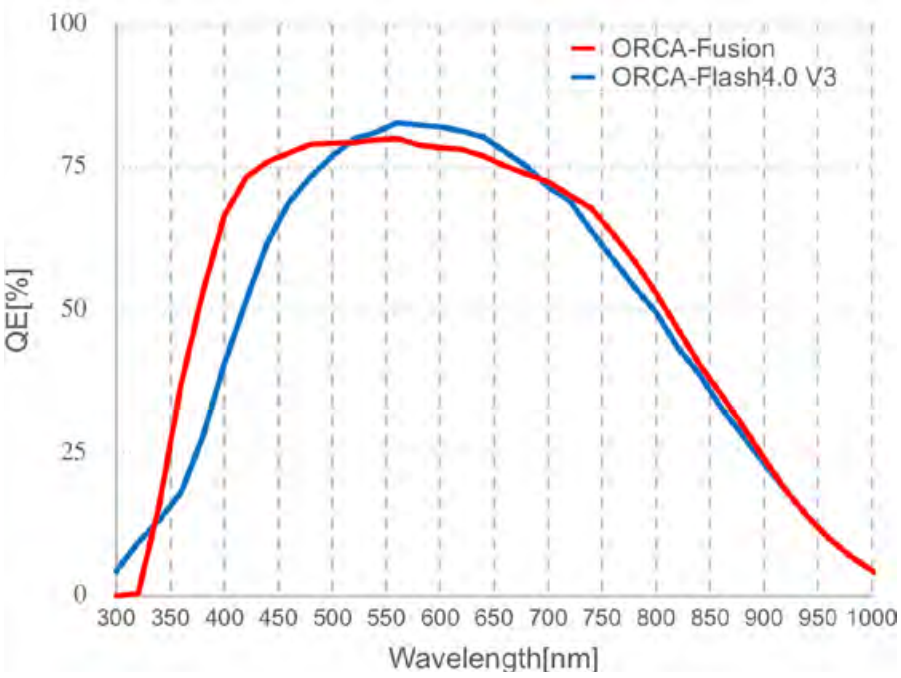

Figure 14. ORCA-Fusion Gen III sensor has high QE from 400-800nm. The high QE of the ORCA-Fusion in combination with low read noise, enables excellent performance in low light conditions.

Special Camera Features of the ORCA-Fusion

Operating temperature and humidity

In a perfect lab environment, the temperature and humidity would be tightly controlled and stable. Unfortunately, this is often not the case especially in labs in tropical and/or humid summer climates. In these conditions, if the room humidity exceeds the operating humidity spec of the camera, the front window of the camera can develop condensation and destroy image quality. To prevent this situation, the ORCA-Fusion was designed with a large operating temperature and humidity range.

Operating temperature	0 to 40 degrees C
Operating humidity	30% to 80% without condensation

Table 4. ORCA-Fusion has wide optimal operating temperature and humidity range. In hot humid conditions, it's possible for condensation to develop on the front window of the camera, ruining image quality. With this wide range of operating conditions, such condensation is unlikely to occur with the ORCA-Fusion.

Vibration and cooling

In a design similar to the ORCA-Flash4.0, the ORCA-Fusion is enabled for either fan or water cooling. In most cases the cooling achieved by the fan is sufficient to reduce the dark current to levels that are insignificant for a given experiment. In some cases, the additional cooling achieved with water circulation is advantageous. However, most water cooling systems are used primarily to eliminate vibration due to the rotation of the fan. The fan vibration of ORCA-Fusion is designed to be sub-pixel level with 100x objective on an inverted microscope. Every microscopy system is different; depending on the needs of the system/experiment, vibration in the ORCA-Fusion can be eliminated with water cooling or suppressed through physical stabilization with an optional base plate.

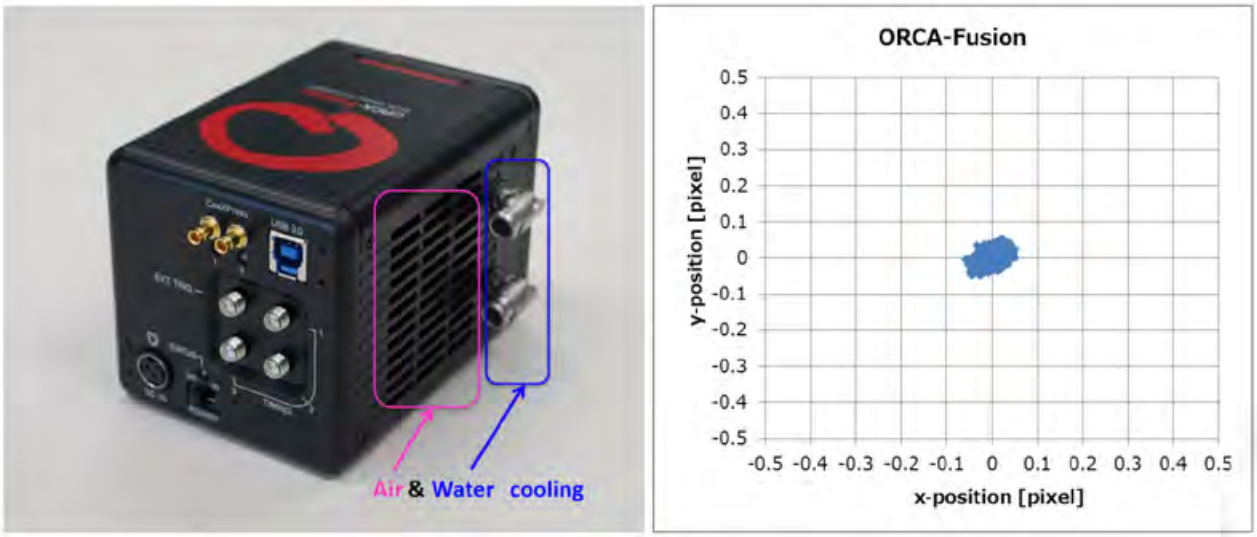

Figure 15. ORCA-Fusion can be operated with air or water cooling. For most applications, air cooling is the simplest and most effective way to achieve optimal dark current and vibration performance. But in some cases, lower dark current or reduced vibration brings additional benefits. The ORCA-Fusion can easily adapt to either need since the connections for water cooling are built into every camera.

CoaXPress and USB3.0

The need to image at speeds higher than 30-40 fps is highly dependent on the experimental conditions and scientific questions. Since high speed imaging comes with additional costs and considerations, the ORCA-Fusion was designed to be versatile. Every ORCA-Fusion can be used with either USB3.0 or CoaXPress. CoaXPress boards and cables can be added at the time of purchase or later as experimental needs evolve. CoaXPress is the state-of-the-art high speed camera interface that enables capturing large quantities of image data quickly. Our DCAM drivers are optimized for either interface and the chart below shows the speed tradeoff for a range of common ROI sizes.

Maximum frame rates					
ROI	Scan mode	CoaXPress	USB3.0		
		16 bit	8 bit	12 bit	16 bit
2,304 x 2,304	Fast	89.1	63.3	42.2	31.6
	Standard	23.2		23.2	
	Ultra-quiet	5.42		5.42	
2,048 x 2,048	Fast	100	80.1	53.4	40.0
	Standard	26.1		26.1	
	Ultra-quiet	6.1		6.1	
256 x 256	Fast	799		799	
	Standard	208		208	
	Ultra-quiet	48.6		48.6	

Figure 16. ORCA-Fusion can run through USB3.0 or CoaXPress. Depending on your experimental needs, you can choose to run the ORCA-Fusion through either CoaXPress or USB3.0 interface. Frame rate differences for the two interfaces are shown at left. Details on the CoaXPress board can be found here.

Read Modes and Triggering Capabilities

A camera is just one piece of a complicated imaging system. To successfully integrate the ORCA-Fusion into many imaging scenarios we offer numerous modes of operation. These modes are defined first by their read out scheme (Normal or Lightsheet) then by the triggering mode (free running or external trigger) and then by the type of external trigger (See Figure 17). The best operation mode is uniquely dependent on the application. The fine timing details of these modes are described in the ORCA-Fusion camera manual and our sales and technical teams are available worldwide to provide customized support.

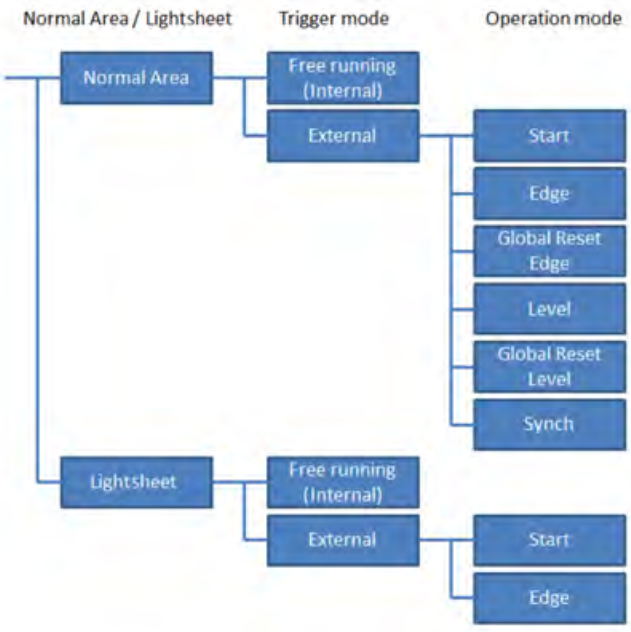

Figure 17. ORCA-Fusion has multiple modes of operation.

DCAM and other software support for the ORCA-Fusion

All Hamamatsu cameras including the ORCA-Fusion are supported by DCAM-API (Digital CAMera Application Programing Inteface), an API that standardizes camera control and functionarity for third party software developers. Currently the ORCA-Fusion is supported in HCImage, LabVIEW, MATLAB and µManager. For additional information on our DCAM and for updates on third party software support of the ORCA-Fusion please see https://dcam-api.com/.

ORCA-Fusion SPECIFICATIONS

Camera	ORCA-Fusion
Product Number	C14440-20UP
Pixel Size	6.5 x 6.5 µm
Effective number of pixels	2304 x 2304
Effective Area	14.976 x 14.976 mm
Readout noise (electrons, rms) *1	
Fast scan	1.4
Standard scan	1.0
Ultra quiet scan	0.7
Quantum efficiency *1	
@ 400 nm	65 %
@ 550 nm	80 %
@ 700 nm	70 %
@ 800 nm	50 %
Full well capacity *1	15,000 electrons
Dynamic range *1	21,400:1 *2
Conversion factor *1	0.24 electrons / count
Cooling Temperature	
With forced-air	-5°C (Ambient temperature: +25°C) *3
Water cooled	-5°C (Water temperature: +25°C) *3
Dark current (electrons/pixel/second) *1	
@ -5°C	0.5
@ -15°C	0.2
Dark offset	100 counts
Dark signal non-uniformity (DSNU)	0.3 electrons rms
Photo response non-uniformity (PRNU)	
@7500 electrons	0.06 % rms
Linearity error *1 **(EMVA 1288 standard)**	0.5 %
Readout modes	Full resolution, digital binning (2 x 2, 4 x 4), sub-array, lightsheet
Readout times at full resolution *4	
Fast scan	11.22 ms (89 fps with CoaXPress or 31.6 fps with USB3.0)
Standard scan	42.99 ms (23.2 fps with CoaXPress or USB3.0)
Ultra quiet scan	184.4 ms (5.4 fps with CoaXPress or USB3.0)
Lightsheet readout (fast scan)	
Row interval time	4.868 µs to 963.8 µs *4
Readout time at full resolution	11.22 ms to 2.221 s *4
Readout modes	Full resolution, sub-array
Readout directions	Top to bottom readout / Bottom to top readout

SPECIFICATIONS CONTINUE

Exposure times	
Fast scan	17 µs ~ 10 s (4.87 µs step)
Standard scan	65 µs ~ 10 s (18.65 µs step)
Ultra quiet scan	280 µs ~ 10 s (80.00 µs step)
Trigger modes	Edge, Level, Sync readout, Start, Global reset edge, Global reset level, programmable
Trigger delay function	Yes
Trigger output	Global exposure timing, trigger ready, low, high
Input trigger connector	SMA x1
Output trigger connectors	SMA x 3
Master pulse mode	Free running / start trigger / burst
Digital output	16 bit [*5] / 12 bit / 8 bit
Interface	CoaXPress (6.25Gbpsx2 lane) and USB3.0 Super Speed [*6]
Lens mount	C-mount (Standard) / F-mount (Part Number TBD)
Software	HCImage, LabVIEW, MATLAB, µManager

Frame Grabber Datasheet: https://dcam-api.com/assets/pdfs/AS-FBD-2XCXP6-2PE8-Hamamatsu.pdf

[*1] Typical value
[*2] Calculated from the ratio of the full well capacity and the readout noise
[*3] Dark current depends on cooling temperature
[*4] Valid to 4 digits and rounded up to 5th digit
[*5] With standard scan, A/D = 14 bits + 2 bits for linearity correction
[*6] USB 3.1 Gen 1 compatible

HAMAMATSU PHOTONICS K.K. www.hamamatsu.com

HAMAMATSU PHOTONICS K.K., Systems Division
812 Joko-cho, Higashi-ku, Hamamatsu City, 431-3196, Japan, Telephone: (81)53-431-0124, Fax: (81)53-435-1574, E-mail: export@sys.hpk.co.jp
U.S.A.: Hamamatsu Corporation: 360 Foothill Road, Bridgewater, NJ 08807, U.S.A., Telephone: (1)908-231-0960, Fax: (1)908-231-1218 E-mail: usa@hamamatsu.com
Germany: Hamamatsu Photonics Deutschland GmbH.: Arzbergerstr. 10, D-82211 Herrsching am Ammersee, Germany, Telephone: (49)8152-375-0, Fax: (49)8152-265-8 E-mail: info@hamamatsu.de
France: Hamamatsu Photonics France S.A.R.L.: 19, Rue du Saule Trapu, Parc du Moulin de Massy, 91882 Massy Cedex, France, Telephone: (33)1 69 53 71 00, Fax: (33)1 69 53 71 10 E-mail: infos@hamamatsu.fr
United Kingdom: Hamamatsu Photonics UK Limited: 2 Howard Court,10 Tewin Road, Welwyn Garden City, Hertfordshire AL7 1BW, UK, Telephone: (44)1707-294888, Fax: (44)1707-325777 E-mail: info@hamamatsu.co.uk
North Europe: Hamamatsu Photonics Norden AB: Torshamnsgatan 35 16440 Kista, Sweden, Telephone: (46)8-509 031 00, Fax: (46)8-509 031 01 E-mail: info@hamamatsu.se
Italy: Hamamatsu Photonics Italia S.r.l.: Strada della Moia, 1 int. 6, 20020 Arese (Milano), Italy, Telephone: (39)02-93 58 17 33, Fax: (39)02-93 58 17 41 E-mail: info@hamamatsu.it
China: Hamamatsu Photonics (China) Co., Ltd.: 1201 Tower B, Jiaming Center, 27 Dongsanhuan Beilu, Chaoyang District, 100020 Beijing, China, Telephone: (86)10-6586-6006, Fax: (86)10-6586-2866 E-mail: hpc@hamamatsu.com.cn
Taiwan: Hamamatsu Photonics Taiwan Co., Ltd.: 8F-3, No.158, Section2, Gongdao 5th Road, East District, Hsinchu, 300, Taiwan R.O.C. Telephone: (886)03-659-0080, Fax: (886)03-659-0081 E-mail: info@hamamatsu.com.tw

Cat. No. SCAS0138E01
OCT/2018 HPK Created in the USA

HAMAMATSU
PHOTON IS OUR BUSINESS